© 2018. Published by The Company of Biologists Ltd | Development (2018) 145, dev159053. doi:10.1242/dev.159053

RESEARCH ARTICLE

The *mir-279/996* cluster represses receptor tyrosine kinase signaling to determine cell fates in the *Drosophila* eye

Hong Duan[1,*], Luis F. de Navas[1,*], Fuqu Hu[1], Kailiang Sun[1,2], Yannis E. Mavromatakis[3], Kayla Viets[4], Cyrus Zhou[4], Joshua Kavaler[5], Robert J. Johnston[4], Andrew Tomlinson[3] and Eric C. Lai[1,‡]

ABSTRACT

Photoreceptors in the crystalline *Drosophila* eye are recruited by receptor tyrosine kinase (RTK)/Ras signaling mediated by Epidermal growth factor receptor (EGFR) and the Sevenless (Sev) receptor. Analyses of an allelic deletion series of the *mir-279/996* locus, along with a panel of modified genomic rescue transgenes, show that *Drosophila* eye patterning depends on both miRNAs. Transcriptional reporter and activity sensor transgenes reveal expression and function of miR-279/996 in non-neural cells of the developing eye. Moreover, *mir-279/996* mutants exhibit substantial numbers of ectopic photoreceptors, particularly of R7, and cone cell loss. These miRNAs restrict RTK signaling in the eye, since *mir-279/996* nulls are dominantly suppressed by positive components of the EGFR pathway and enhanced by heterozygosity for an EGFR repressor. miR-279/996 limit photoreceptor recruitment by targeting multiple positive RTK/Ras signaling components that promote photoreceptor/R7 specification. Strikingly, deletion of *mir-279/996* sufficiently derepresses RTK/Ras signaling so as to rescue a population of R7 cells in R7-specific RTK null mutants *boss* and *sev*, which otherwise completely lack this cell fate. Altogether, we reveal a rare setting of developmental cell specification that involves substantial miRNA control.

KEY WORDS: *Drosophila*, R7 photoreceptor, RTK signaling, MicroRNA

INTRODUCTION

The *Drosophila* eye is a choice model system for studying cell fate specification owing to its highly stereotyped array of pattern elements. Each eye consists of ∼800 ommatidial units, each of which contains eight photoreceptors of distinct identities, four cone cells, and about eight pigment cells; a mechanosensory bristle organ develops at alternate ommatidial vertices. The orderly acquisition of cell fates during eye development is coordinated by multiple signaling pathways and transcription factors (Kumar, 2012).

Initially, a proneural zone defined by the basic helix-loop-helix activator Atonal is resolved into single R8 photoreceptors by Notch pathway signaling. Each R8 nucleates a developing ommatidium, and a stepwise set of events mediated by Epidermal growth factor receptor (EGFR) and receptor tyrosine kinase (RTK) signaling progressively recruit the R2/5, R3/R4, R1/6 and R7 photoreceptors to each ommatidial cluster (Freeman, 1996). A specialized RTK signal transduced by the Sevenless (Sev) receptor specifies the final photoreceptor, R7. In parallel to EGFR and Sev signaling, Notch signaling defines photoreceptor subtypes (Cagan and Ready, 1989). Further non-sensory cell fates are subsequently recruited to each ommatidial cluster, including cone cells followed by primary and secondary pigment cells.

The existence of extensive regulatory networks mediated by microRNAs (miRNAs) suggests broad possibilities for their requirement during development or physiology (Flynt and Lai, 2008; Sun and Lai, 2013). As is true for most tissues, loss of core miRNA biogenesis factors such as Dicer-1 or Pasha causes substantial defects in the developing *Drosophila* eye (Lee et al., 2004; Smibert et al., 2011). Beyond the general requirement for miRNA biogenesis in this tissue, some individual miRNAs and miRNA sites influence eye development. For example, studies of the hypermorphic *Enhancer of split m8*^{D} [*E(spl)m8*^{D}] allele revealed its post-transcriptional repression by K box motifs (Lai et al., 1998) – indeed long before these were recognized as binding sites for K box family miRNAs (Lai, 2002; Lai et al., 2005). Specific mutation of K boxes from an *E(spl)m8* genomic transgene sensitizes the *Notch*^{split} background, yielding a synthetic, smaller rough eye (Lai et al., 1998). The bantam miRNA is required for the growth and proliferation of all imaginal discs; thus, loss of bantam reduces eye tissue and increases apoptosis (Brennecke et al., 2003; Hipfner et al., 2002). The *mir-263a/b* loci are essential for development of eye interommatidial bristles, and protect the shaft cells of these sensory organs from apoptosis (Hardiman et al., 2002; Hilgers et al., 2010).

By contrast, many other *Drosophila* miRNAs connected to eye development lack substantial defects when mutated on their own, but are sensitive to genetic background or environmental stress. For example, miR-7 positively regulates photoreceptor specification by repressing the neural inhibitor *yan* (*aop*), a transcriptional repressor in the EGFR pathway (Li and Carthew, 2005). Although deletion of *mir-7* alone has only minor effects on eye development, its deletion sensitizes the eye to alteration in EGFR signaling (Li and Carthew, 2005) or temperature fluctuation (Li et al., 2009). Similarly, deletion of *mir-11*, located in the intron of *E2f1*, does not have substantial effects by itself, but this condition renders the eye sensitive to E2F1-dependent, DNA damage-induced apoptosis (Truscott et al., 2011). These and other examples have led to the notion that miRNAs are primarily important for robustness, but are individually mostly dispensable for normal developmental programs.

In this study, we elucidate crucial roles for the *mir-279/996* locus during *Drosophila* eye development. These seed-related miRNAs

[1]Department of Developmental Biology, Sloan-Kettering Institute, 1275 York Ave, Box 252, New York, NY 10065, USA. [2]Program in Neuroscience, Weill Cornell Medical College, New York, NY 10065, USA. [3]Department of Genetics and Development, College of Physicians and Surgeons, Columbia University, 701 West 168th Street, New York, NY 10032, USA. [4]Department of Biology, Johns Hopkins University, 3400 N. Charles Street, Baltimore, MD 21218, USA. [5]Department of Biology, Colby College, Waterville, ME 04901, USA.
*These authors contributed equally to this work

‡Author for correspondence (laie@mskcc.org)

E.C.L., 0000-0002-8432-5851

Received 5 September 2017; Accepted 28 February 2018

Development (2018) 145, dev159053. doi:10.1242/dev.159053

are expressed from an operon and are functionally equivalent in several neural settings (Sun et al., 2015), including during suppression of CO_2 neurons (Cayirlioglu et al., 2008; Hartl et al., 2011), control of circadian behavior (Luo and Sehgal, 2012), and control of mechanosensory organ development (Kavaler et al., 2018). We now show that these miRNAs are deployed in non-neuronal cells of the developing eye, and their deletion strongly alters eye cell fates, yielding ectopic photoreceptors and loss of cone cells. Focusing on ectopic R7 photoreceptors, we use genetic interactions to demonstrate that miR-279/996 restrict RTK/Ras signaling, which normally promotes R7 specification. This is attributable to their direct repression of multiple positive components of RTK signaling pathways. Strikingly, the efficacy of endogenous *mir-279/996* in restricting RTK/Ras signaling is substantial enough that deletion of these miRNAs can rescue a population of R7 photoreceptors in the absence of the Boss ligand or the Sev receptor.

These findings highlight how a single miRNA locus can exert phenotypically substantial, and not merely fine-tuning, roles in multiple biological settings. Moreover, these miRNAs achieve similar functional roles (neural repression) through mechanistically distinct strategies (i.e. by repressing RTK/Ras components in the eye, by repressing a Notch inhibitor in mechanosensory organs, or by repressing transcription factors in the olfactory system).

RESULTS

The *mir-279/996* locus is essential for normal eye development

The seed-related *mir-279* and *mir-996* were previously considered to be expressed from independent transcription units, with *mir-279* being solely required in various developmental settings (Cayirlioglu et al., 2008; Luo and Sehgal, 2012; Yoon et al., 2011). However, we recently clarified that these miRNAs are functionally overlapping and co-expressed as an operon, and that '*mir-279*-specific' deletions also impair the expression of miR-996 (Sun et al., 2015). Our key genetic reagents include hypomorphic and null alleles of the *mir-279/996* operon, and wild-type and modified genomic transgenes expressing only miR-279 or miR-996 (Fig. 1A).

In our search for novel *mir-279/996* functions, we observed that our mutants exhibit defects in the normally crystalline adult eye (Fig. 1B). Taking advantage of our allelic series, we found that the severity of eye roughening is exacerbated by decreasing dosage of *mir-279/996* (Fig. 1C-F). The phenotypes of *mir-279/996[15C/15C]* double-deletion homozygotes were rescued by a 16.6 kb *mir-279/996* genomic transgene, demonstrating that the eye defects are due to loss of this miRNA locus (Fig. 1G). Moreover, sole expression of either miR-279 or miR-996 from the same genomic context restored normal adult eyes to *[15C/15C]* null animals (Fig. 1H,I). Thus, these miRNAs exhibit substantial functional redundancy across diverse *in vivo* settings (Sun et al., 2015).

To gain initial insight into underlying defects caused by lack of miR-279/996, we sectioned adult eyes of various heteroallelelic mutants. Normal eyes exhibit seven of the eight photoreceptor rhabdomeres in a given section (Fig. 1J), arranged as six large outer photoreceptors (R1-6) surrounding a small inner photoreceptor (R7/8, depending on the apical-basal position of the section). Notably, all three mutant combinations examined showed ectopic outer and inner photoreceptors (Fig. 1K-M). Based on the position and morphology of the latter, the ectopic inner photoreceptors were preferentially R7. We annotated representative sections according to the key in Fig. 1, with circles of different colors indicating ommatidia with one or more outer R cells, and arrowheads designating ectopic R7 cells. Fig. 1N-R shows magnifications of individual normal and mutant ommatidia, and highlights the variety of abnormal photoreceptor combinations present in *mir-279/996* heteroallelic eyes. Quantification revealed that the strong mutant combination *ex36/15C* exhibited stronger defects than either hypomorphic combination examined, and >21% of ommatidia in *ex36/15C* exhibited ectopic photoreceptors (Fig. 1S). Notably, although there are eight photoreceptor subtypes, these quantitative analyses indicate that a majority of mutant ommatidia in all three transheterozygous backgrounds examined exhibit ectopic R7 cells. Thus, specification of the R7 photoreceptor appears particularly sensitive to the miRNAs.

Overall, these data reveal that defective allocation of cell fates contributes to eye roughening in *mir-279/996* mutants, and that both miRNAs are required for normal eye development. We note that although the eye is sensitive in revealing developmental abnormalities, it is actually rare for miRNA mutants to exhibit retinal phenotypes. Indeed, in a recent survey of new deletion alleles covering ∼100 *Drosophila* miRNAs, including most operons analyzed as cluster knockouts, only one novel locus (*mir-92a*) affected eye morphology and barely any others discernibly affected external development (Chen et al., 2014). Therefore, these eye specification defects in *mir-279/996* mutants represent some of the most overt developmental phenotypes detected among miRNA mutants.

Transcriptional activity of *mir-279/996* in the pupal eye

We examined the spatial expression of miR-279/996 in the developing eye. We generated a transcriptional reporter in which cytoplasmic GFP was knocked into a 16.6 kb genomic fragment that extends into the flanking upstream and downstream protein-coding genes (Fig. 2A). This genomic fragment provides full rescue of *mir-279/996* function in multiple settings (Sun et al., 2015), including during eye development (Fig. 1G-I), indicating that it contains all relevant cis-regulatory information.

In eyes staged at 45 h after puparium formation (APF), the differentiation of all ommatidial cell types has occurred, and they have adopted their appropriate relative positions in the mature unit eye. The nuclei of the different cell types adopt characteristic locations along this axis, and can be divided into four layers (Fig. 2B). Most apically lie the quartet of cone cell nuclei, below which are the nuclei of the paired primary pigment cells. The third level is made from the eight photoreceptor nuclei, and most basally lie the nuclei of the secondary/tertiary pigment cells and the bristle cells. The *mir-279/996-GFP* reporter is expressed throughout the cone and primary pigment cell layer [as marked by expression of nuclear DPax2 (Shaven), Fig. 2C], as well as in the accessory pigment and bristle cells, but is clearly excluded from photoreceptors (as marked by nuclear Elav, Fig. 2D,E). Therefore, this miRNA locus is deployed in multiple non-neuronal eye cell types, but is excluded from photoreceptors.

Endogenous activity of miR-279/996 in non-neural cells of the pupal eye

As some miRNAs are regulated post-transcriptionally, patterned expression of the *mir-279/996-GFP* reporter does not necessarily equate to their spatial activity. We therefore generated a miRNA activity sensor, composed of a ubiquitously expressed GFP reporter bearing two sequences complementary to miR-279 (Fig. 2A). In theory, this *tub-GFP-miR-279* transgene should be repressed by both miR-279 (via RNAi) and miR-996 (via miRNA seed matching). Interestingly, expression of the *tub-GFP-miR-279*

Development (2018) 145, dev159053. doi:10.1242/dev.159053

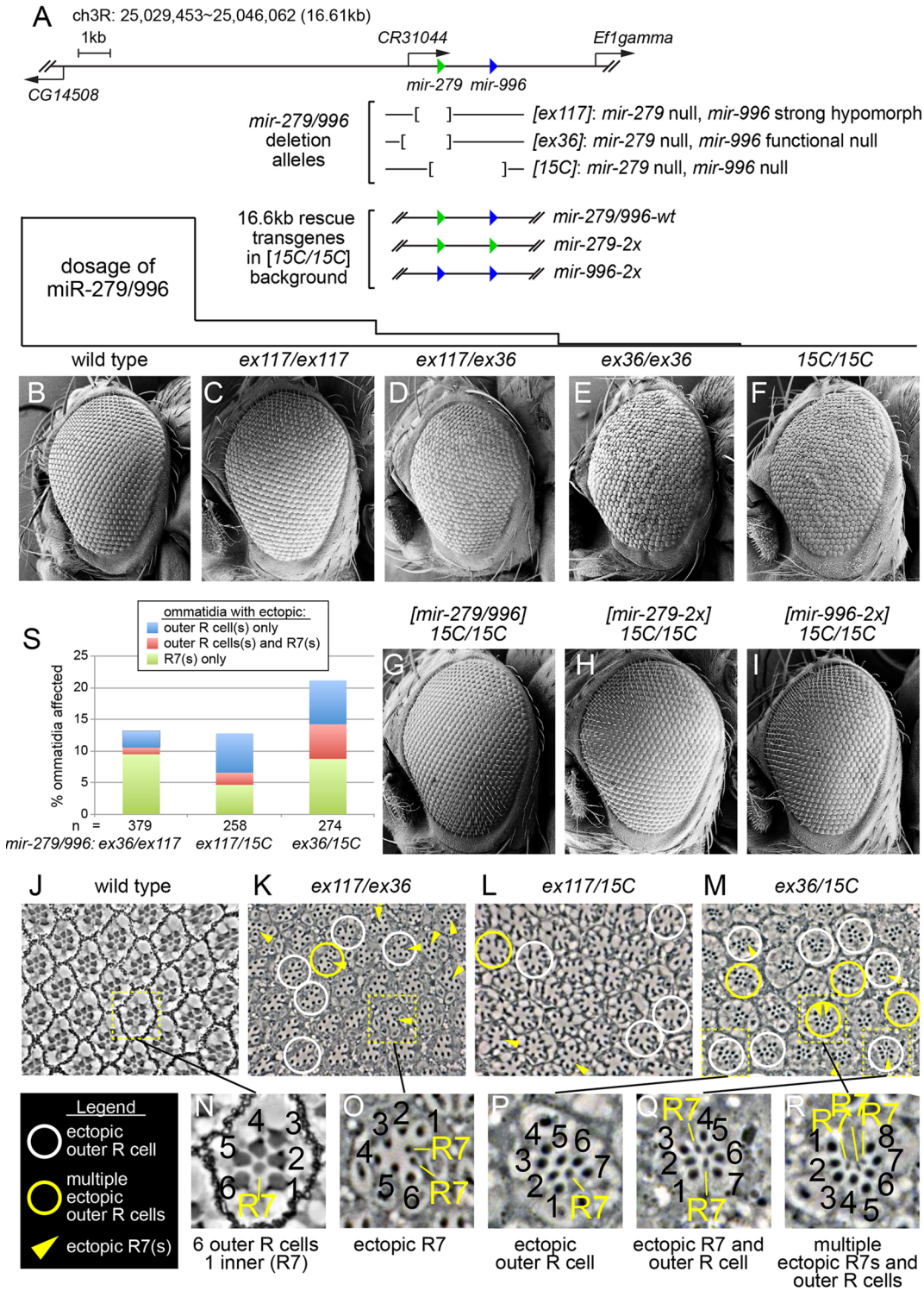

Fig. 1. *mir-279/996* alleles and corresponding adult *Drosophila* eye phenotypes. (A) The *Drosophila mir-279/996* genomic region, along with three deletion alleles and three rescue transgenes built into a 16.6 kb genomic backbone. (B-I) Adult *Drosophila* eyes analyzed by scanning electron microscopy. (B) The wild-type eye exhibits a regular, crystalline organization. (C) A hypomorphic condition that is deleted for *mir-279* and is impaired for miR-996 biogenesis appears externally normal, whereas genotypes that progressively remove miR-279/996 activity exhibit overt roughening and ommatidial disorganization (D-F). (G-I) The exterior eye phenotype caused by deletion of both *mir-279* and *mir-996* (in *[15C]* homozygotes) can be rescued by supplying both miRNAs (G), only *mir-279* (H) or only *mir-996* (I). (J-M) Plastic sections through adult eyes of wild type (J) and three heteroallelic *mir-279/996* combinations (K-M). Normal ommatidia exhibit six large outer photoreceptor rhabdomeres (R1-6) surrounding a smaller inner photoreceptor rhabdomere (R7 or R8, depending on the apical-basal position). All of the transheterozygous *mir-279/996* mutants exhibit populations of ommatidia with ectopic outer and/or inner photoreceptors, as annotated in the key to the left. Based on their position and morphology, the ectopic inner photoreceptors are predominantly R7. Some ommatidia can contain both ectopic outer and R7 photoreceptors, and the frequency of mutant ommatidia is noticeably higher in the strongest mutant transheterozygote *ex36/15C* (M). (N-R) Magnifications of individual ommatidia highlighting normal and different combinations of mutant photoreceptor identities. (S) Quantification of photoreceptor subtypes in the three heteroallelic *mir-279/996* mutants examined. R7 is the predominant photoreceptor subtype affected in all genotypes.

Development (2018) 145, dev159053. doi:10.1242/dev.159053

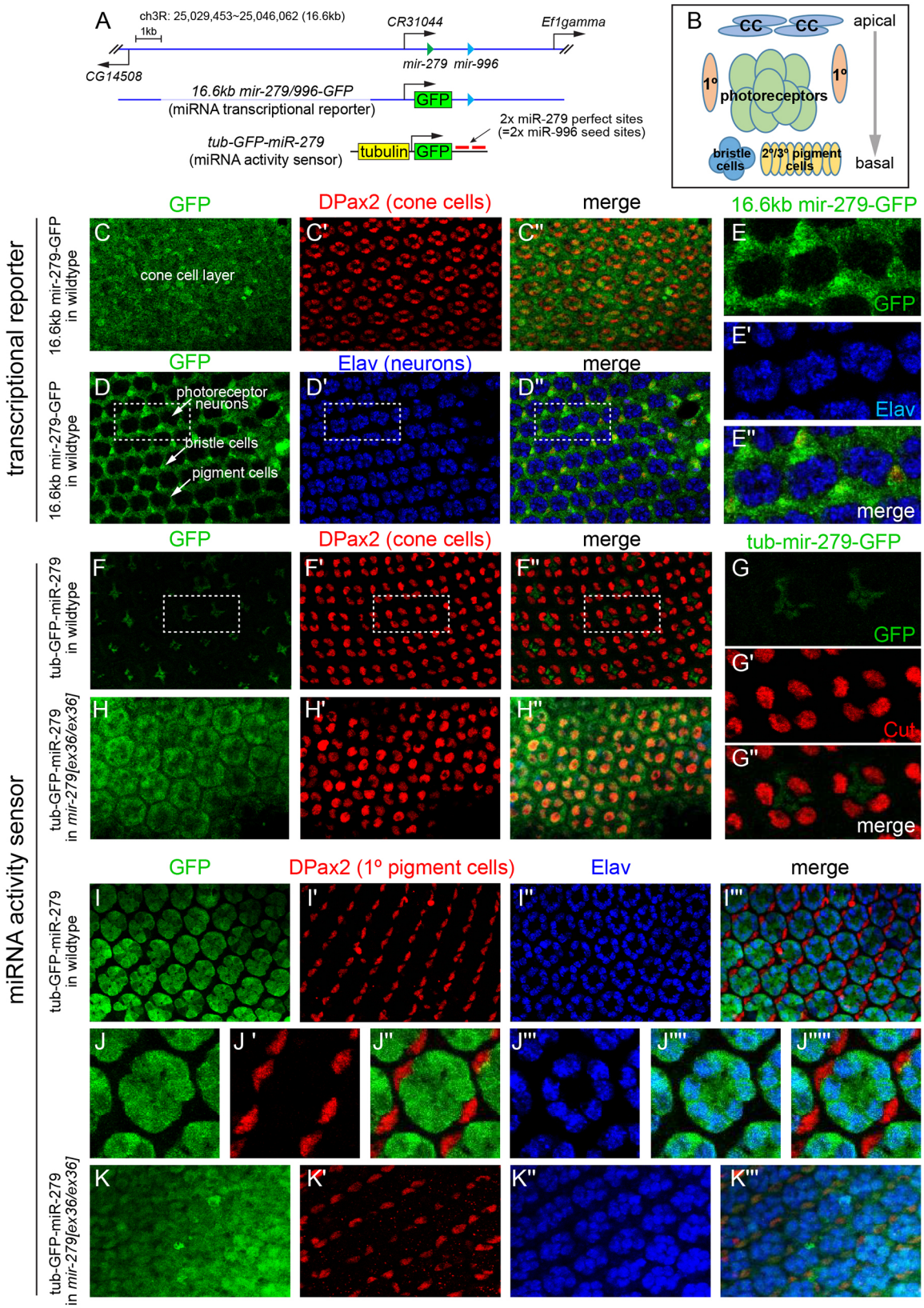

Fig. 2. See next page for legend.

sensor was complementary to that of the transcriptional reporter; sensor GFP expression was robust in photoreceptor cells, but absent in cone cells, pigment cells and the non-neuronal cells of interommatidial bristle organs (Fig. 2F,G,I). The non-neuronal activity of miR-279/996 was particularly apparent at higher magnification of photoreceptor and primary pigment cells, since

Development (2018) 145, dev159053. doi:10.1242/dev.159053

Fig. 2. Expression and activity of *mir-279/996* in the developing pupal eye. (A) Transgenes to detect transcriptional activity or functional repression by *mir-279/996*; the former is a positive readout of miRNA expression, whereas the latter is a negative sensor of miRNA activity. (B) Schematic of ommatidial nuclei in the fly eye. Cone cell (CC) nuclei are located most apically, primary pigment cells and photoreceptors reside medially, and secondary and tertiary pigment cells and interommatidial bristle nuclei are located basally. (C-E″) Expression of the 16.6 kb *mir-279/996-GFP* transgene is readily detected throughout the cone cell layer as marked by DPax2 (C) and in the pigment cells and bristle cells (D), but is excluded from Elav$^+$ photoreceptor neurons. (E) Magnification of the boxed region in D, highlighting exclusion of *mir-279/996-GFP* activity from Elav$^+$ cells. (F-K‴) Functional repression detected by the *tub-GFP-miR-279* sensor. Note that this is a cytoplasmic sensor, whereas the cell-specific markers are nuclear. (F) The *tub-GFP-miR-279* sensor is largely excluded from the cone cell layer. (G) Magnified view of the boxed region in F. (H) The *tub-GFP-miR-279* sensor is reactivated in cone cells when placed in the *mir-279/996[ex36/ex36]* background. (I) The *tub-GFP-miR-279* sensor is coincident with Elav$^+$ photoreceptors but is excluded from pigment cells. (J-J⁗) Higher magnification view emphasizing the on and off spatial pattern of the miR-279 sensor in adjacent Elav$^+$ and DPax2$^+$ cells, respectively. (K-K‴) The *tub-GFP-miR-279* sensor is reactivated in non-neuronal cells within the photoreceptor plane of *mir-279/996[ex36/ex36]* mutants.

GFP was specifically absent from DPax2$^+$ primary pigment cells that are directly adjacent to Elav$^+$ photoreceptors (Fig. 2J).

If the non-uniform expression of the *tub-GFP-miR-279* sensor is truly imposed by these miRNAs, its spatial activity should become equalized in *mir-279/996* mutants. Indeed, expression of the *tub-GFP-miR-279* sensor became uniform throughout the cone cells (Fig. 2H) and the pigment and bristle cells (Fig. 2K) of *mir-279/996[15C/15C]* eyes. We conclude that the *mir-279/996* locus is not only transcriptionally active, but also mediates strong functional repression within diverse non-neuronal cells of the developing eye.

miR-279/996 are required for normal specification of ommatidial cell fates

We characterized the cellular bases of adult eye patterning defects in *mir-279/996* mutants (Fig. 1), which were already becoming evident during the course of our expression pattern studies (Fig. 2). We initially used antibodies to the adherens junctions component Armadillo (Arm). Arm stains throughout the apical surface of photoreceptor cells at 36 h APF, but becomes restricted to zonula adherens junctions by 45 h APF (Zelhof and Hardy, 2004). At the latter time point, Arm staining at the *z*-level in which the photoreceptor apices are well separated reveals seven structures, as R8 resides basally to the others (Fig. 3A). Deletion of *mir-279/996* increased the number of Arm$^+$ photoreceptors observed in single confocal sections (Fig. 3B). These phenotypes were rescued by presence of the wild-type transgene, indicating that they result from the loss of *mir-279/996* (Fig. 3C). Defects were also evident at the cone cell layer, where Arm staining normally outlines the four cone cells in each ommatidia. By contrast, *mir-279/996* mutant ommatidia frequently contained only three cone cells, a phenotype that was also rescued by the wild-type transgene (Fig. 3D-F).

Although the distribution of abnormal ommatidia could be stronger in certain areas of a given eye, there did not appear to be a reproducible spatial preference (e.g. dorsal/ventral or central/peripheral) of phenotypes among eyes. Therefore, to quantify these defects, we utilized all available tissue from all pupal eye preparations. We note that occasional ommatidia exhibited six photoreceptors in a section; however, this did not prove to genuinely reflect photoreceptor loss. Careful examination in confocal stacks revealed these to be due to disturbed cell arrangements, since other photoreceptor apices could be found at other *z*-levels (Fig. S1). Overall, ∼20% of ommatidia have one or two extra photoreceptors in *mir-279/996[15C/15C]* (Fig. 3G), which corresponds to the quantifications from adult sections (Fig. 1). In addition, ∼25% of ommatidia were missing one or two cone cells (Fig. 3H), with a very minor frequency (0.68%) exhibiting five cone cells. The wild-type genomic transgene fully rescued both the ectopic photoreceptor and missing cone cell phenotypes.

We confirmed the cone cell and photoreceptor defects using other markers. We used Discs large (Dlg, or Dlg1) to label cell membranes and DPax2 to label cone cells, and confirmed a substantial population of three-cone ommatidia; these defects were rescuable (Fig. 3I-K). We then analyzed the general neuronal marker Elav to assess over-recruitment of R cells. Although quantification of Elav is challenging due to its diffuse immunoreactivity and the fact that photoreceptor nuclei do not all reside at the same *z*-level at mid-pupal stages, we clearly observed ommatidia with ectopic Elav$^+$ cells in *mir-279/996* mutants (Fig. 3L-N). By carefully examining cells along the *z*-axis in confocal stacks, we confirmed that wild-type ommatidia are associated with eight DAPI-stained Elav$^+$ photoreceptor nuclei, while all ommatidia exhibiting supernumerary photoreceptors with Arm staining carried a correlating increase of DAPI-stained Elav$^+$ nuclei (Fig. S1). This excludes the possibility that ectopic Arm$^+$ structures simply reflect mispositioning of R8, and demonstrates that the miRNA mutants develop ectopic photoreceptors.

Finally, we examined the effects of ectopically expressing *mir-279/996* in the photoreceptors. We first used *GMR-Gal4* to drive expression of *UAS-DsRed-mir-279* in all cells of the developing retina. This treatment strongly disrupted the retina, making it challenging to monitor any cell fate changes. We therefore used the more restricted driver *sev-Gal4*, which is active in R3/R4, R1/R6, R7 and cone cells. Adult eyes of *sev-Gal4; UAS-DsRed-mir-279* showed a selective effect in the R3/4 photoreceptors, which were often degenerate with missing or vestigial rhabdomeres (Fig. S2). Although it is unclear why R3/4 are preferentially sensitive to ectopic *mir-279*, this result suggests that elevated miR-279 can interfere with photoreceptor formation.

miR-279/996 are predominantly required to restrict R7 photoreceptor fate

To gain insight into the identity of ectopic photoreceptors in *mir-279/996* null mutants, we examined a panel of cell-specific markers. At 45 h APF, we observed two classes of supernumerary photoreceptors. Staining for Sens (R8) and BarH1 (R1/6) revealed a low frequency of photoreceptors of heterogeneous fate (Fig. S3). By contrast, staining for the R7 marker Prospero (Pros) revealed a substantial population of ommatidia with two, and sometimes three, Pros$^+$ cells; these were fully suppressed by the genomic *mir-279/996* transgene (Fig. 3O-Q). These cells colabeled with Elav, indicating that they are photoreceptors. Some retinal regions showed much higher densities of the ectopic Pros$^+$ cells than others (Fig. 3R). However, as we could not assign any specific area of the retina that was consistently more affected, our quantifications utilized all available tissue across samples. This revealed that ∼10% of 45 h APF ommatidia bear supernumerary Pros$^+$ cells (Fig. 3S), confirming that R7 comprises a dominant subclass of the ectopic photoreceptors induced by the loss of *mir-279/996*. This supports our morphological classifications and quantifications from adult sections (Fig. 1J-S).

To determine whether mid-pupal cells that ectopically express Pros indeed differentiate as R7s, we stained for the R7-specific rhodopsins

Development (2018) 145, dev159053. doi:10.1242/dev.159053

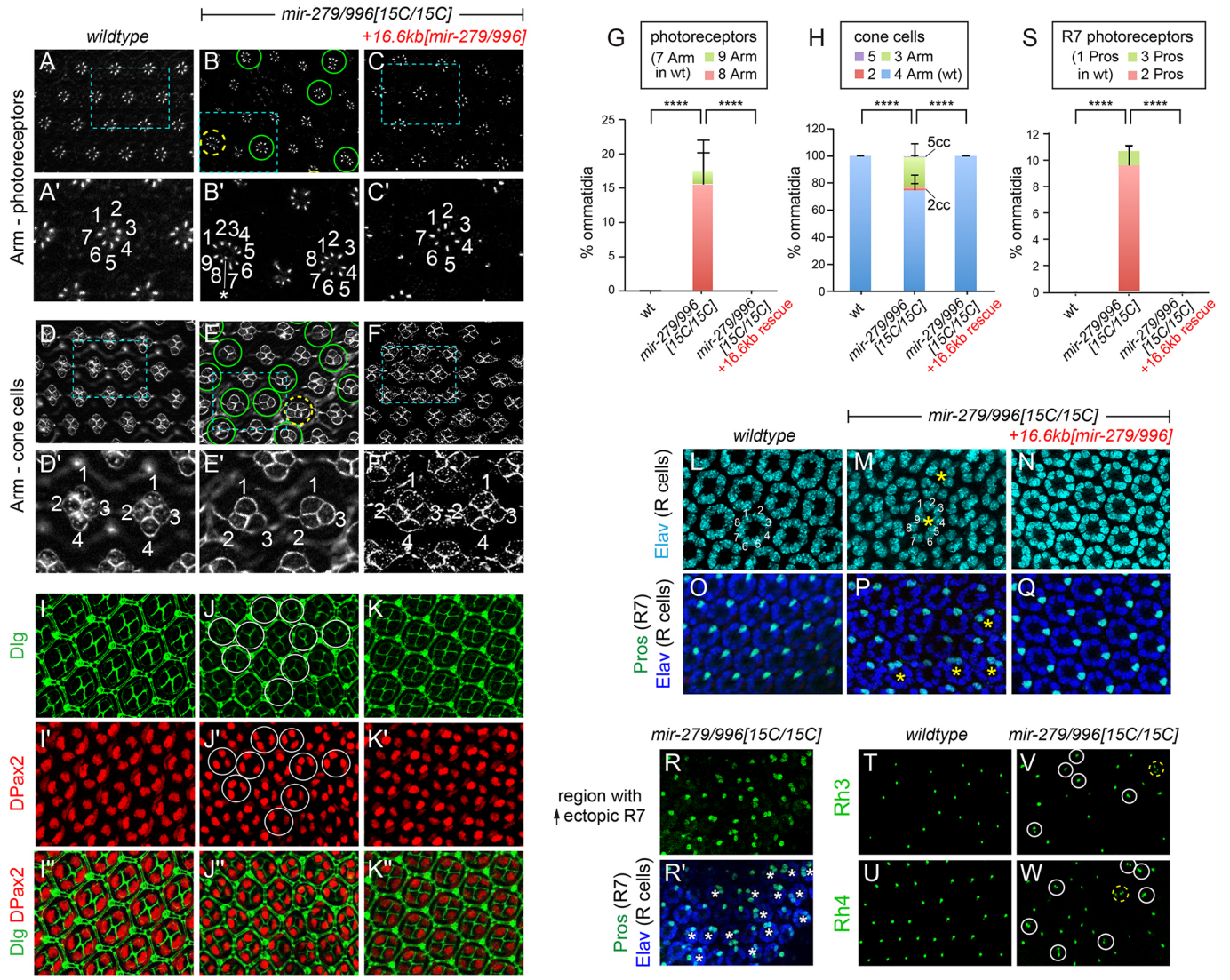

Fig. 3. Cell specification defects in *mir-279/996* mutant eyes. Stainings and quantifications in A-S were from ∼45 h APF pupal eyes, while stainings in T-W were from adult eyes. (A-F) Arm labels the zonula adherens of apically constricted photoreceptors. (A) Seven of the eight neurons are labeled by Arm in a single optical section at the *z*-level in which the photoreceptor apices are well separated. (B) *15C* homozygotes frequently have supernumerary photoreceptors, with ommatidia bearing eight Arm$^+$ photoreceptors in a single optical section (green circles), and occasionally more (the yellow circle indicates an ommatidium with nine or possibly ten photoreceptors). (C) These defects were suppressed by a 16.6 kb *mir-279/996* genomic transgene. (A′-C′) Higher magnifications of individual ommatidial groups (boxed regions in A-C) with photoreceptors labeled. A potential tenth photoreceptor in B′ is indicated with an asterisk. (D) In the cone cell layer, Arm labels groups of four cones in each wild-type ommatidium. (E) *mir-279/996[15C/15C]* mutants frequently have only three (or even two) cone cells (circles); very rarely, five cone cell clusters are seen (yellow circle). (F) Cone cell defects are fully rescued by the genomic transgene. (D′-F′) Higher magnifications of individual ommatidial groups (boxed regions in D-F) with cone cells labeled. (G,H) Quantification of ommatidia with aberrant photoreceptor number (G) or cone cell number (H) in *mir-279/996* mutants and rescues. Error bars indicate s.d. ****P<0.0001, one-way ANOVA with Tukey's HSD post-hoc test. (I-K″) Co-staining for Dlg (green, cell membranes) and DPax2 (red, cone cell nuclei). (I) The regular pattern of four cone cells per ommatidium is seen in wild type (wt). (J) *mir-279/996[15C/15C]* mutants frequently exhibit three cone cells per ommatidium, which is rescued by a genomic transgene (K). (L-N) Staining for the neuronal marker Elav demonstrates mutant ommatidia with ectopic photoreceptors (asterisks). (O-Q) Co-staining for Elav and Pros shows that many ectopic photoreceptors are R7 cells. (R,R′) Region of *mir-279/996* mutant eye that shows an especially high frequency of ectopic Pros photoreceptors (asterisks). (S) Quantification of ommatidia with ectopic Pros$^+$ R7 cells. Error bars indicate s.d. ****P<0.0001, one-way ANOVA with Tukey's HSD post-hoc test. (T-W) Staining for rhodopsins selectively expressed in terminally differentiated R7 cells: Rh3 (T,V) and Rh4 (U,W). *mir-279/996* mutant ommatidia are labeled; white circles indicate two R7 cells and yellow circles indicate three R7 cells.

Rh3 and Rh4 in adult eyes. Their expression is stochastic, but mutually exclusive, within mature R7 neurons and thus defines two functional subclasses (Fig. 3T,U). We observed ∼12.7% of ommatidia with ectopic Rh3 and/or Rh4 staining (Fig. 3V,W), concordant with the results of ectopic Pros reactivity at 45 h APF. We further analyzed Pros expression in the genetic combinations *mir-279/996[15C/ex36]* and *[ex117/ex117]* (Fig. 1A). These exhibited 8.8% and 1.7% of ommatidia with ectopic Pros$^+$ cells, respectively, consistent with the fact that these different *mir-279* deletions express lower and higher levels of miR-996, respectively (Sun et al., 2015). Finally, rescue experiments with *mir-279*-only and *mir-996*-only genomic transgenes showed that both could completely rescue ommatidial cellular organization in the *15C* null homozygotes, including full suppression of ectopic Pros$^+$ cells (Fig. S4).

Overall, these cytological tests validate observations from the adult that defective mutant eye phenotypes are a direct consequence

Development (2018) 145, dev159053. doi:10.1242/dev.159053

of miRNA loss, and that both miR-279 and miR-996 can direct normal eye patterning and neuronal suppression.

miR-279/996 repress multiple positive RTK/Ras signaling factors

Supernumerary photoreceptors typically result from ectopic activation of RTK/Ras signaling. As the photoreceptor subtype most sensitive to endogenous *mir-279/996* was R7, we focused our efforts on understanding its specification. Two RTKs are active in *Drosophila* eye development: EGFR and the Sev receptor (Hafen et al., 1987; Schejter and Shilo, 1989). Ectopic activation of either RTK, or their downstream pathways, will trigger cone cell precursors to adopt the R7 fate (Basler et al., 1991). Strikingly, multiple positive core components of the EGFR and Sev signaling pathways bear highly conserved miR-279/996 seed matches in their 3′ UTRs (Fig. 4A). These include *rhomboid* (*rho*) and *roughoid* (*ru*, also known as *rho3*), which encode two serine-type endopeptidases that generate active EGFR ligands, and *bride of sevenless* (*boss*), which encodes the ligand for the Sev receptor. The sites in *ru* and *boss* are optimal ‘8mer’ sites, whereas the site in *rho* is a 7mer-1A site (Lewis et al., 2005). All of these sites are conserved in all sequenced drosophilids, indicating that they are under strong selective constraint (Fig. 4A,B).

We used luciferase sensor assays in cultured cells (Sun et al., 2015) to demonstrate that the 3′ UTRs of RTK pathway factors can be repressed by miR-279 and miR-996. We first tested a validated sensor for the key miR-279 target *nerfin-1* (Cayirlioglu et al., 2008) and observed nearly 90% reduction. We show here that miR-996 has similar activity to miR-279 (Fig. 4C). *nerfin-1* is an unusually strong miRNA target due to five conserved matches to the same miRNA seed, a number that few fly mRNAs bear. By comparison, we observed reduction by half to two-thirds in the levels of the *rho*, *ru* and *boss* 3′ UTR sensors (Fig. 4C), which is comparable to more ‘typical’ miRNA targets. To demonstrate direct regulation, we mutated the cognate binding sites. This abrogated the response of the *rho*, *ru* and *boss* 3′ UTR sensors, indicating that regulation is mediated directly via individual miR-279/996 seed matches (Fig. 4C).

We next generated *tubulin-GFP* transgenes to the full 3′ UTRs of these RTK signaling genes and examined their regulation in the fly. When a control transgene was crossed into a background expressing *UAS-DsRed-mir-279* using *ptc-Gal4*, the expression of the miRNA can be marked in DsRed^{+} cells, which do not alter GFP expression (Fig. 4D). However, when the three RTK pathway sensor transgenes were assayed, all three were cell-autonomously suppressed in the miRNA-expressing domain (Fig. 4E-G). Therefore, *rho*, *ru* and

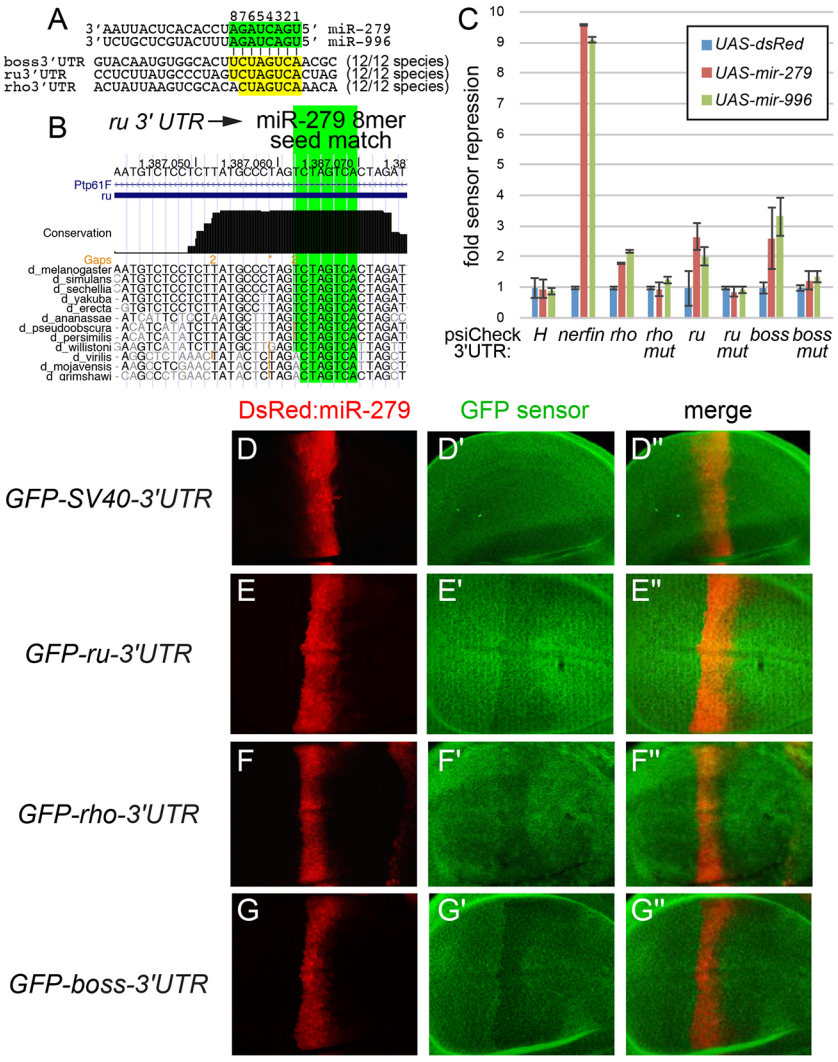

Fig. 4. miR-279/996 directly repress multiple positive components of RTK/Ras pathways. (A) Among 3′ UTRs bearing target sites for the shared miR-279/996 seed sequence, three (*ru*, *rho*, *boss*) are positive components of RTK/Ras that promote photoreceptor/R7 specification. *rho* bears a 7mer-1A site, whereas *boss* and *ru* both contain high-affinity 8mer sites. (B) All of these sites are conserved across the 12 sequenced *Drosophila* genomes, as exemplified for *ru*. (C) Luciferase sensor assays demonstrate target 3′ UTR repression by miR-279 and miR-996. *Hairless* (*H*) is used as a negative control, while *nerfin-1* is a positive control that is exceptionally well repressed by both miRNAs. *rho*, *ru* and *boss* are repressed 2- to 3-fold by ectopic miR-279/996 in a seed-dependent manner. Error bars indicate s.d. (D-G″) Evidence that miR-279 represses Ras pathway 3′ UTRs *in vivo*. Shown are the central portions of wing imaginal discs that express GFP ubiquitously (*tub-GFP-3′ UTR* sensors), in a genetic background in which miR-279 is ectopically expressed in a central stripe labeled by DsRed. (D) miR-279 does not affect a control GFP sensor, but induces cell-autonomous repression of GFP sensors linked to *ru* (E), *rho* (F) and *boss* (G) 3′ UTRs.

Development (2018) 145, dev159053. doi:10.1242/dev.159053

boss are bona fide targets of these miRNAs. These results provide *in vitro* and *in vivo* evidence for post-transcriptional regulation of multiple positive components of RTK/Ras signaling by miR-279/996.

miR-279/996 represses RTK/Ras signaling during eye development

We sought to connect the action of the miRNAs on RTK signaling to the phenotypes observed in *mir-279/996* mutant eyes by assaying for dominant genetic interactions. Even though miRNAs typically have large cohorts of conserved targets (at least 130 *Drosophila* genes bear conserved 3′ UTR seed matches for miR-279/996, http://www.targetscan.org), at least some miRNA mutant phenotypes are highly dose sensitive on the level of individual targets. This implies that particular genes or pathways, out of the entire target network, may drive a particular miRNA mutant phenotype (Dai et al., 2012).

Both Nerfin-1 and Escargot (Esg) are key miR-279 targets, and their heterozygosity can suppress the specification of ectopic CO_2-sensing neurons in the miRNA mutants (Cayirlioglu et al., 2008; Hartl et al., 2011). However, heterozygosity for neither *nerfin-1* nor *esg* modulated the eye roughening of *mir-279/996[15C]* homozygous eyes; in fact, double heterozygosity for these target genes did not suppress eye roughening of the miRNA deletion (Fig. 5A-C). This suggests that the miR-279/996 target cohort that is crucial in olfactory system development is not substantially required during eye development.

Since the ectopic R7s likely resulted from ectopic activation of the RTK pathway, and many RTK-associated genes are functionally targeted by miR-279/996, we next examined genetic interactions with genes associated with RTK activation. Notably, heterozygosity for *Egfr*, *ru*, *rho*, and the nuclear effector *phyllopod* (*phyl*), each yielded detectable dominant suppression of overall adult eye roughness (Fig. 5D-F). The strongest individual suppression was observed with heterozygosity for *phyl*, which was not predicted as a direct miR-279/996 target. However, as a nuclear component of the RTK/Ras pathway, Phyl integrates signaling from both EGFR and Sev signaling, and was previously isolated by virtue of its strong dominant suppression of an activated Ras phenotype (Chang et al., 1995; Dickson et al., 1995). Nevertheless, to test whether combined loss of direct targets could produce greater suppression, we generated a *ru, rho, 15C* recombinant chromosome and backcrossed this to *mir-279/996[15C]*. Double heterozygosity for *ru* and *rho* strongly rescued the regularity of *[15C/15C]* external eyes (Fig. 5G).

We examined the cellular basis of these morphological rescues. Arm staining at 45 h APF served as a convenient readout of photoreceptor numbers. Indeed, multiple components of the EGFR/Ras pathway dominantly suppressed the frequency of ommatidia with ectopic photoreceptors (Fig. 5H-L). We extended these interaction tests by examining the secreted EGFR inhibitor Argos (Freeman et al., 1992; Schweitzer et al., 1995). Whereas *argos* heterozygotes (*argos/+*) were normal in an otherwise wild-type background, *argos/+* enhanced ectopic photoreceptors in *mir-279/996[15C]* mutants (Fig. 5M).

We recapitulated these findings by specific analysis of R7 cells. In particular, double heterozygosity of *nerfin-1* and *esg* did not modify the number of $Pros^+$ cells (Fig. 5N), further indicating that dominant phenotypic suppression is not a trivial genetic outcome, even among demonstrated 'crucial' miRNA targets. On the other hand, heterozygosity for multiple positive EGFR/Ras pathway components (e.g. *ru*, *rho* and *phyl*) each reduced R7 cell numbers (Fig. 5O-R), whereas heterozygosity for *argos* strongly increased R7 cells (Fig. 5S).

We quantified the nature of these genetic interactions at the level of cell fate readouts. Analyses of photoreceptor numbers (Arm^+ cells, Fig. 5T) and R7 photoreceptors ($Pros^+/Elav^+$ cells, Fig. 5U) validated the magnitude and directionality of these phenotypic modifications, and provide further evidence that miR-279/996 endogenously suppress Ras/RTK signaling during eye development. Importantly, assignment of miRNA control of R7 specification extended to terminal differentiation. Supernumerary R7 photoreceptors expressing Rh3 or Rh4 were reduced to <2% in *ru, rho* double heterozygotes, and to ∼0.5% in *phyl* heterozygotes. Reciprocally, whereas *argos* heterozygotes did not exhibit ectopic R7 cells (Fig. 5U), *argos* dominantly enhanced their presence in 15C homozygotes (Fig. 5V). Even with the caveat that the morphological aberration of some rhabdomeres interfered with assignment of photoreceptor subtype, at least 31.6% of ommatidia in *argos/+, mir-279/996[15C/15C]* eyes carried an unambiguously ectopic R7 cell.

Finally, we examined interactions with *boss*. Although the R7 phenotypes we observed could relate to the activities of either EGFR or Sev, and *boss* is a functional miR-279/996 target, we did not detect substantial genetic interactions of *boss* heterozygotes with *mir-279/996[15C]* homozygotes (Fig. 5U). Failure to observe a dominant effect does not rule out the involvement of Boss/Sev signaling. Nevertheless, the strong genetic interactions of *mir-279/996* mutants with positive and negative Ras pathway factors suggest that the phenotype preferentially relates to secretion and antagonism of the EGFR ligand.

Deletion of *mir-279/996* partially bypasses Boss and Sev for R7 specification

The R7 precursor is unusual in that it requires potent activation of the RTK/Ras pathway, an activation level that EGFR alone cannot supply (Tomlinson et al., 2011). Instead, activation of both EGFR and Sev is required, and if Sev alone is removed all ommatidia lack R7s, as this cell transforms into an equatorial cone cell (Tomlinson and Ready, 1986) (Fig. 6A,B). We therefore extended the previous heterozygote experiments by investigating the effect of full *mir-279/996* loss-of-function in the *sev* null background. In particular, we were interested whether EGFR pathway activation caused by lack of *mir-279/996* might restore R7 differentiation in the absence of Sev.

We sectioned adult eyes of *mir-279/996[15C/ex36]* transheterozygotes in a *sev[d2]* background. Whereas *sev[d2]* does not differentiate any R7s, concomitant loss of *mir-279/996* yielded a striking population of rescued R7s (Fig. 6C). We note that in *sev* mutant ommatidia the R8 cell can migrate into the apical regions and present a central rhabdomere that can be mistaken for an R7. To ensure that the rescued cells were bona fide R7s, we examined the basal regions of the R7-bearing ommatidia in adjacent sections, and confirmed the presence of the endogenous R8 (Fig. 6C′). Since the rescued R7s reside in the appropriate position, the simplest scenario is that the equatorial cone cell has been transformed into R7, as opposed to one of the other three cone cell types.

We next examined *sev* and *sev; mir-279/996* double-mutant eyes in 45 h pupae. As expected, *sev* mutants completely lack $Pros^+$ R7 cells (Fig. 6D). We were able to confirm that the antibody staining was successful since the $Pros^+$ sheath cells of the interommatidial bristle sensory organs were labeled. Sheath cells do not express Elav and are thus distinct from the $Elav^+$ neurons of these bristle organs (Fig. 6D′,D″). By contrast, *sev; mir-279/996* double mutants differentiated a population of $Pros^+$ R7 cells, which were confirmed as photoreceptors since they colabeled with Elav (Fig. 6E).

Development (2018) 145, dev159053. doi:10.1242/dev.159053

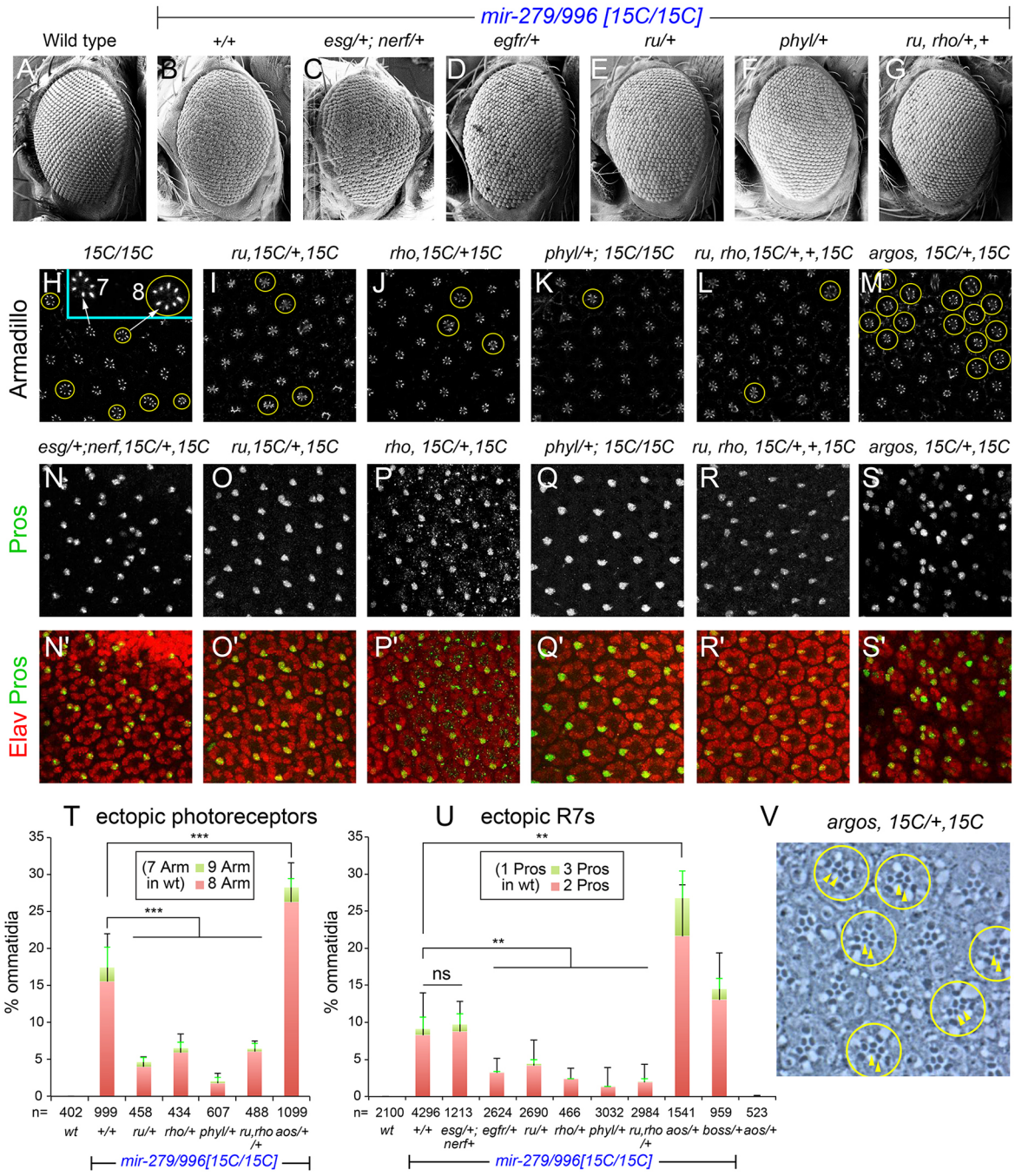

Fig. 5. *mir-279/996* mutant phenotypes are due to elevated Ras pathway activity. Except for the wild-type eye (A), all other adult and pupal eye samples are homozygous for *mir-279/996[15C]*, with other heterozygous mutations as indicated. (A-G) Scanning electron microscopy of adult eyes. (A) Normal regular arrangement of wild-type ommatidia. The rough eye of the *mir-279/996[15C]* homozygote (B) is not modified by double heterozygosity for *nerfin-1* and *esg* (C), but is partially suppressed by *Egfr*/+ (D) and *ru*/+ (E), and strongly suppressed by *phyl*/+ (F) and *ru, rho*/+, + (G). (H-S′) 45 h APF eyes stained for the indicated markers. (H-M) Arm staining focused on photoreceptor apices. Mutant ommatidia with ectopic photoreceptors (eight in one optical section) are circled; the inset (H) shows examples of ommatidia with seven and eight photoreceptors at higher magnification. The phenotype of *[15C/15C]* (H) is dominantly suppressed by heterozygosity for positive Ras pathway components (I-L) and dominantly enhanced by *argos*, a Ras pathway inhibitor (M). (N-S) Pros (green) and Elav (red) staining to detect R7 cells. The phenotype of *[15C/15C]* is not substantially modified by double heterozygosity for *nerfin-1* and *esg* (N), but is dominantly suppressed by heterozygosity for positive Ras pathway components (O-R) and dominantly enhanced by *argos* (S). (T,U) Quantification of ectopic photoreceptor (T) and ectopic R7 (U) phenotypes in various genotypes. Error bars indicate s.d. ***P*<0.01, ****P*<0.001, one-way ANOVA with Tukey's post-hoc test. (V) Retinal section of *argos, 15C/15C* adult eye illustrates a high frequency of ectopic R7 cells (arrowheads), which can be identified based on their central position within the circled ommatidia.

Similar to *sev* mutants, loss of *boss* function ablates R7 specification (Fig. 6F). By contrast, *boss[1], mir-279/996[15C]* double homozygotes displayed clear rescue of a population of Pros^{+} photoreceptors in R7 positions (Fig. 6G). We quantified the restoration of Pros^{+} R7 cells to *sev* and *boss* mutants by concomitant loss of *mir-279/996* (Fig. 6H). Overall, these data provide striking evidence for endogenous restriction of EGFR pathway activity by these miRNAs, which constitute novel crucial players in one of the classic paradigms of cell fate specification.

Development (2018) 145, dev159053. doi:10.1242/dev.159053

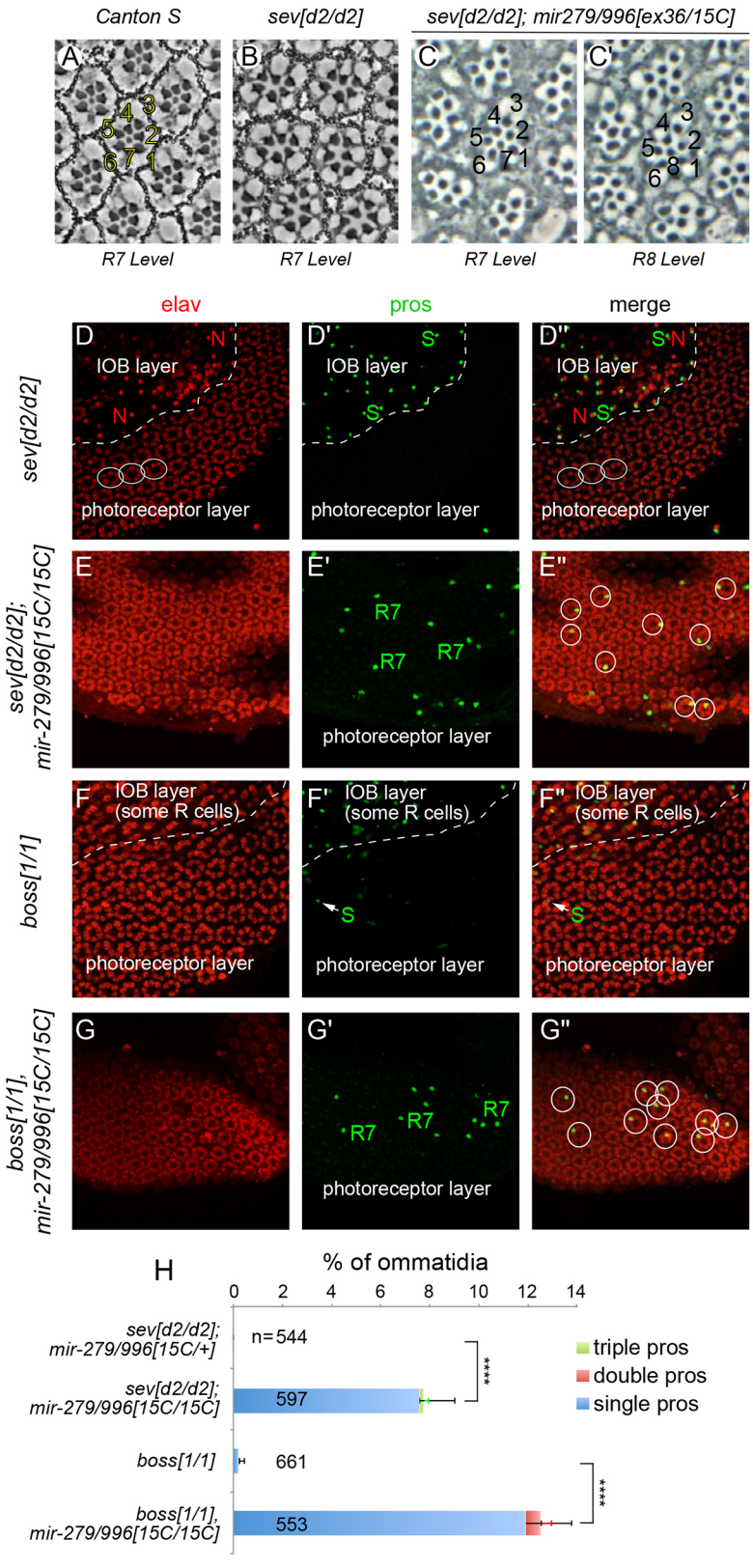

Fig. 6. Deletion of *mir-279/996* partially rescues R7 cells in *sev* and *boss* mutants. (A-C) Plastic sections of adult eyes. (A) Section of Canton S at the R7 cell level shows the characteristic trapezoidal arrangement of seven photoreceptor rhabdomeres in each ommatidia. (B) Section of *sev[d2]* mutant shows only six photoreceptors, with the centrally located R7 absent. (C) Example of rescued R7 cell in *sev[d2]; mir-279/996[ex36/15C]* eye; an adjacent section from the R8 level confirms the presence of R8 (C′), demonstrating that the cell assigned as R7 is not a misplaced R8. (D-G″) Double staining for Pros (green) and Elav (red) at 45 h APF. (D) *sev* mutant eye lacks Pros$^+$ photoreceptors. Proper staining is confirmed by including a section that overlaps the interommatidial bristle (IOB) layer, where adjacent pairs of Pros$^+$ sheath (S) and Elav$^+$ neuronal (N) cells are present in each IOB organ. (E) *sev; mir-279/996* double-mutant eye shows presence of Pros$^+$ (R7) cells; their identity as photoreceptors is evidenced by colabeling for Elav (circled in E″). (F) *boss* mutant eye lacks Pros$^+$ photoreceptors. (G) *boss, mir-279/996* double-mutant eye exhibits rescue of a population of R7 cells (circled in G″). (H) Quantification of R7 rescue in *sev* and *boss* mutants by concomitant deletion of *mir-279/996*. Error bars indicate s.d. ****P<0.0001, one-way ANOVA with Tukey's post-hoc test.

DISCUSSION

miR-279/996 and eye development

During *Drosophila* eye development, the level of RTK pathway activation determines whether a cell can adopt the photoreceptor fate. Multiple mechanisms, including activation of Notch (Tomlinson et al., 2011) and release of Argos (Freeman et al., 1992), ensure that the pathway is activated only in presumptive photoreceptors. Here, we presented molecular and genetic evidence indicating that miR-279/996 suppress RTK activation in non-photoreceptor cells during eye development. Of note, the fact that

Development (2018) 145, dev159053. doi:10.1242/dev.159053

mir-279/996 mutants exhibit a rich set of reciprocal genetic interactions with positive and negative Ras pathway factors suggests that this locus might have unknowingly been hit in previous large-scale dominant modifier screens in the *Drosophila* eye used to isolate components of the RTK pathway (Karim et al., 1996; Simon et al., 1991).

Supernumerary photoreceptors typically result from ectopic activation of RTK/Ras signaling in either of two groups of cells that are not normally destined to become photoreceptors (Basler et al., 1991). Mystery cells are constituents of the early ommatidia that are subsequently lost from the structure (Tomlinson and Ready, 1987). However, if their RTK/Ras pathway is activated, they can generate supernumerary photoreceptors of the R1-6 class (with large rhabdomeres). Cone cells are added to developing ommatidia after the photoreceptors. If RTK/Ras signaling is inappropriately activated in these cells, they generate photoreceptors of the R7 class (with small rhabdomeres) (Basler et al., 1991). As we observe substantial populations of excess photoreceptors with large as well as small rhabdomeres in *mir-279/996* mutants, our data are consistent with the occurrence of both mystery cell transformations and cone cell transformations, although we have focused on the latter as the inferred source of ectopic R7 cells. Further studies are needed to characterize the basis and subtypes of other photoreceptor transformations in *mir-279/996* mutants.

The two RTKs active in *Drosophila* eye development, Sev and EGFR, share intracellular transduction pathways but differ markedly in their ligands. Boss is the ligand for Sev and is an integral plasma membrane protein, whereas Spitz, the ligand for EGFR, is a diffusible peptide released by a subset of differentiating photoreceptors. Although we identify *boss* as a conserved and functional miR-279/996 target, our genetic experiments do not yet implicate miR-279/996 as restricting Boss/Sev signaling. Instead, the data are consistent with the scenario that miR-279/996 may regulate the presentation of ligands to EGFR. In particular, genes that positively regulate EGFR ligands (*ru* and *rho*) are both conserved targets and dominant suppressors of *mir-279/996* mutant eye phenotypes.

One of the most striking phenotypic readouts in *mir-279/996* mutants is the fact that a subset of R7 cells can be rescued by deletion of the miRNA locus in *boss* or *sev* mutants. It is well documented that directed misexpression of activated Ras pathway components can rescue R7 cells in Sev pathway mutants (Basler et al., 1991; Fortini et al., 1992). However, there are very few loss-of-function mutants that can rescue R7 cells in *boss* or *sev* mutants. Mutations of the Ras target gene inhibitor Yan (Lai and Rubin, 1992) and the neural inhibitor Ttk (Lai et al., 1996; Xiong and Montell, 1993) can induce R7 photoreceptors in *sev* mutants, but mutation of the Ras pathway inhibitor Argos does not (Freeman et al., 1992). Of note, the H214 enhancer trap (Mlodzik et al., 1992) is selectively active in R7 precursors and not other photoreceptors. In the absence of *sev*, the R7 precursor transforms into a cone cell precursor and yet retains H214 expression. This was the first evidence that the R7 precursor could receive positional information independently of Sev. Whether H214 expression relates to miR-279/996 activity, and whether it responds to the Notch signals that the R7 precursor receives, remains to be investigated.

Overall, the endogenous impact of miR-279/996 in the eye is more profound than the typical view of 'fine-tuning' regulation attributed to most miRNAs. Indeed, the eye phenotypes of *mir-279/996* mutants place it among a small cohort of miRNA mutants in any species that, when deleted, have overt consequences on external morphology and assignment of cell fate. Although the miR-279 family is not found in chordates (Mohammed et al., 2014), its genetic attributes might have relevance to cancer mechanisms. The setting-specific nature of *mir-279/996* mutant phenotypes provides precedent that potential human miRNA deletions that unleash Ras signaling in disease and cancer might await genetic discovery.

Multiple developmental roles for miR-279/996

A striking dichotomy has emerged from the genetic analysis of miRNA biology (Lai, 2015). The founding miRNAs and even miRNA target sites were identified from genetic aberrations of miRNA loci and 3′ UTRs that yielded highly penetrant morphological defects. Alongside bioinformatic and molecular evidence that miRNAs target a majority of animal transcriptomes, it is widely considered that miRNAs have broad impacts on gene expression. On the other hand, systematic collections of miRNA deletions demonstrate that the vast majority do not cause seemingly overt phenotypes (Chen et al., 2014; Miska et al., 2007). Thus, miRNA loci were probably historically undersampled not on account of the small mutational target size of mature miRNAs, but rather because they only rarely exhibit notable phenotypes that would have permitted their isolation from forward genetic screens.

This dichotomy is intensified by the fact that among the minority of miRNAs with overt phenotypic impacts, several are involved in distinct biological processes, often via different target outputs (Smibert and Lai, 2010). In this regard, *mir-279/996* is an exemplar of a highly pleiotropic miRNA locus. Forward genetic screening originally identified a crucial role for miR-279, later extended to miR-996, in preventing CO_2-sensing olfactory neuron development from maxillary palps (Cayirlioglu et al., 2008; Sun et al., 2015). In this setting, the miRNAs repress neural transcription factors encoded by *nerfin-1* and *esg* to restrict CO_2-responsive neurons (Cayirlioglu et al., 2008; Hartl et al., 2011). Additional studies revealed that these miRNAs control different aspects of JAK-STAT signaling. In the CNS, repression of the JAK-STAT ligand Unpaired is important for circadian behavior (Luo and Sehgal, 2012), whereas regulation of the STAT transcription factor influences ovarian border cell dynamics (Monahan and Starz-Gaiano, 2013; Yoon et al., 2011). Most recently, we found that miR-279/996 suppress neuronal specification in the mechanosensory lineage by repressing the Notch inhibitor Insensible (Kavaler et al., 2018). Here, we extend the role of miR-279/996 to suppressing photoreceptor specification by limiting EGFR/Ras signaling. Notably, the ectopic neuron phenotypes in the olfactory lineage, mechanosensory lineage, and the eye are genetically dose sensitive to distinct target cohorts, and might thus represent convergent 'anti-neural' outputs for this miRNA operon.

MATERIALS AND METHODS

Drosophila strains

We used our published *mir-279/996* alleles *[ex117]*, *[ex36]* and *[15C]*, the genomic 16.6 kb transgenes of *mir-279/996*, *mir-279-2x* and *mir-996-2x* (Sun et al., 2015), and *UAS-DsRed-mir-279* (Bejarano et al., 2012). Other alleles and stocks utilized were: *ru[1]* (BDSC #575), *rho[ve-1]* (BDSC #628), *su(ve)[1] ru[1] rho[ve-1] h[1] th[1]* (BDSC #617), *argos[rlt]* (BDSC #7336), *phyl[2245]-SR2-3* (G. Rubin, Janelia Farm, VA, USA), *Egfr[f24]* (A. Simcox, Ohio State University, OH, USA), *boss[1]* (H. Kramer, UT Southwestern, TX, USA), *nerfin-1[54]* (W. Odenwald, NIH, Washington DC, USA) and *sev[d2]* (A. Tomlinson, Columbia University, NY, USA). Appropriate recombinants were constructed to assay genetic interactions with *mir-279/996* alleles.

To generate the *mir-279-GFP* transgene, we used recombineering to retrieve genomic fragments of 11.8 kb upstream and of 4.7 kb downstream of the *mir-279* hairpin from the BAC CH322-35G11 (BACPAC Resources)

Development (2018) 145, dev159053. doi:10.1242/dev.159053

and cloned them between the *Asc*I and *Not*I sites of attB-P[acman]-Amp^R (H. Bellen, Baylor College of Medicine, TX, USA). *hsp70-GFP-SV40* was PCR cloned from the pEGFP vector (Brennecke et al., 2003) and inserted into the 5′ end of the 4.7 kb genomic fragment, then the resultant EGFP +4.7 kb piece was digested out and ligated with the 11.8 kb upstream sequence to generate the 16.6 kb *mir-279-GFP* construct. Transgenic flies were generated using the PhiC31 system (BestGene).

We generated transgenic sensors by cloning two complementary sequences to miR-279, or the 3′ UTRs of *rho*, *ru*, *boss* and *neur*, downstream of *tub-GFP*. The 3′ UTRs were amplified from genomic DNA using the primers listed in Table S1, and cloned into the *Xba*I/*Xho*I sites of *tub-GFP*. Transgenic animals were generated by co-injection with Δ2-3 helper plasmid (gift of G. Rubin).

Immunohistochemistry

We used a standard protocol for immunostaining of imaginal discs (Lai and Rubin, 2001). Primary antibodies were rat anti-Elav (1:30, 7E8A10, DSHB), mouse anti-Cut (1:25, 2B10, DSHB), mouse anti-Prospero (1:20, MR1A, DSHB), mouse anti-Dlg (1:100, 4F3, DSHB), rabbit anti-DPax2 [1:2000; gift of J. Kavaler (Kavaler et al., 2018)], rabbit anti-GFP (1:1250, A-11122, Invitrogen), chicken anti-GFP (1:1000, ab13970, Abcam), mouse anti-Rh3 (1:10; gift of S. Britt, University of Colorado), rabbit anti-Rh4 (1:100; gift of C. Zuker, Columbia University), rabbit anti-BarH1 (1:500; gift of Kwang-Wook Choi, KAIST South Korea) and guinea pig anti-Senseless (1:2500; gift of Hugo Bellen, Baylor College of Medicine). We used appropriate secondary antibodies conjugated to Alexa 488, 568 and 647 (1:500, Molecular Probes).

Luciferase sensor assays

We used previously described luciferase 3′ UTR sensors in the psiCheck2 backbone for *nerfin-1*, *ru*, *rho* and *boss* (Sun et al., 2015). Point mutations in miR-279/996 seed matches were introduced by site-directed mutagenesis with the oligonucleotides listed in Table S1 and confirmed by sequencing.

S2 cells were plated in 96-well plates and transfected with 12.5 ng/well either UAS-DsRed empty vector or UAS-DsRed-miRNA constructs, 12.5 ng/well psiCheck2 plasmid and 6.25 ng/well ub-Gal4. Transfections were performed using Effectene Transfection Reagent (Qiagen) according to the manufacturer's instructions. Luciferase values were measured 3 days after transfection. We normalized transfection efficiencies using control firefly luciferase carried within psiCheck2, and fold repression was normalized against empty UAS-DsRed and empty psiCheck2 plasmid. We present representative data from quadruplicate sensor assays, for which each set was performed at least three times and found to yield qualitatively similar results. The S2 cells were recently authenticated as being male cells based on expression of the male *Sxl* transcript isoform but were not tested for other contamination.

Acknowledgements

We thank the Bloomington *Drosophila* Stock Center (BDSC), the Developmental Studies Hybridoma Bank (DSHB), and numerous colleagues (cited in the Materials and Methods) for providing fly stocks and antibodies.

Competing interests

The authors declare no competing or financial interests.

Author contributions

Conceptualization: H.D., E.C.L.; Methodology: H.D., R.J.J., A.T., E.C.L.; Validation: H.D., L.F.d.N.; Formal analysis: H.D., L.F.d.N., F.H., Y.E.M., K.V., C.Z., J.K., A.T.; Investigation: H.D., L.F.d.N., F.H., K.S., Y.E.M., K.V., C.Z., A.T.; Resources: H.D., F.H., K.S.; Data curation: H.D., L.F.d.N., K.V., C.Z., J.K., E.C.L.; Writing - original draft: E.C.L.; Writing - review & editing: R.J.J., A.T., E.C.L.; Visualization: H.D., L.F.d.N., E.C.L.; Supervision: R.J.J., A.T., E.C.L.; Project administration: E.C.L.; Funding acquisition: E.C.L.

Funding

Work in the R.J.J. group is supported by National Institutes of Health (NIH) R01-EY025598. Work in the A.T. group was supported by NIH R01-EY026217. Work in the E.C.L. group was supported by the Burroughs Wellcome Fund and the NIH (R01-NS074037, R01-NS083833 and R01-GM083300) and Memorial Sloan-Kettering Cancer Center core grant P30-CA008748. Deposited in PMC for release after 12 months.

Supplementary information

Supplementary information available online at
http://dev.biologists.org/lookup/doi/10.1242/dev.159053.supplemental

References

Basler, K., Christen, B. and Hafen, E. (1991). Ligand-independent activation of the sevenless receptor tyrosine kinase changes the fate of cells in the developing Drosophila eye. *Cell* **64**, 1069-1081.

Bejarano, F., Bortolamiol-Becet, D., Dai, Q., Sun, K., Saj, A., Chou, Y.-T., Raleigh, D. R., Kim, K., Ni, J.-Q., Duan, H. et al. (2012). A genome-wide transgenic resource for conditional expression of Drosophila microRNAs. *Development* **139**, 2821-2831.

Brennecke, J., Hipfner, D. R., Stark, A., Russell, R. B. and Cohen, S. M. (2003). *bantam* encodes a developmentally regulated microRNA that controls cell proliferation and regulates the proapoptotic gene *hid* in *Drosophila*. *Cell* **113**, 25-36.

Cagan, R. L. and Ready, D. F. (1989). *Notch* is required for successive cell decisions in the developing *Drosophila* retina. *Genes Dev.* **3**, 1099-1112.

Cayirlioglu, P., Kadow, I. G., Zhan, X., Okamura, K., Suh, G. S., Gunning, D., Lai, E. C. and Zipursky, S. L. (2008). Hybrid neurons in a microRNA mutant are putative evolutionary intermediates in insect CO_2 sensory systems. *Science* **319**, 1256-1260.

Chang, H. C., Solomon, N. M., Wassarman, D. A., Karim, F. D., Therrien, M., Rubin, G. M. and Wolff, T. (1995). phyllopod functions in the fate determination of a subset of photoreceptors in Drosophila. *Cell* **80**, 463-472.

Chen, Y.-W., Song, S., Weng, R., Verma, P., Kugler, J.-M., Buescher, M., Rouam, S. and Cohen, S. M. (2014). Systematic study of Drosophila microRNA functions using a collection of targeted knockout mutations. *Dev. Cell* **31**, 784-800.

Dai, Q., Smibert, P. and Lai, E. C. (2012). Exploiting Drosophila genetics to understand microRNA function and regulation. *Curr. Top. Dev. Biol.* **99**, 201-235.

Dickson, B. J., Domínguez, M., van der Straten, A. and Hafen, E. (1995). Control of Drosophila photoreceptor cell fates by phyllopod, a novel nuclear protein acting downstream of the Raf kinase. *Cell* **80**, 453-462.

Flynt, A. S. and Lai, E. C. (2008). Biological principles of microRNA-mediated regulation: shared themes amid diversity. *Nat. Rev. Genet.* **9**, 831-842.

Fortini, M. E., Simon, M. A. and Rubin, G. M. (1992). Signalling by the sevenless protein tyrosine kinase is mimicked by Ras1 activation. *Nature* **355**, 559-561.

Freeman, M. (1996). Reiterative use of the EGF receptor triggers differentiation of all cell types in the Drosophila eye. *Cell* **87**, 651-660.

Freeman, M., Klämbt, C., Goodman, C. S. and Rubin, G. M. (1992). The argos gene encodes a diffusible factor that regulates cell fate decisions in the Drosophila eye. *Cell* **69**, 963-975.

Hafen, E., Basler, K., Edstroem, J. E. and Rubin, G. M. (1987). Sevenless, a cell-specific homeotic gene of Drosophila, encodes a putative transmembrane receptor with a tyrosine kinase domain. *Science* **236**, 55-63.

Hardiman, K. E., Brewster, R., Khan, S. M., Deo, M. and Bodmer, R. (2002). The bereft gene, a potential target of the neural selector gene cut, contributes to bristle morphogenesis. *Genetics* **161**, 231-247.

Hartl, M., Loschek, L. F., Stephan, D., Siju, K. P., Knappmeyer, C. and Kadow, I. C. (2011). A new Prospero and microRNA-279 pathway restricts CO_2 receptor neuron formation. *J. Neurosci.* **31**, 15660-15673.

Hilgers, V., Bushati, N. and Cohen, S. M. (2010). Drosophila microRNAs 263a/b confer robustness during development by protecting nascent sense organs from apoptosis. *PLoS Biol.* **8**, e1000396.

Hipfner, D. R., Weigmann, K. and Cohen, S. M. (2002). The bantam gene regulates Drosophila growth. *Genetics* **161**, 1527-1537.

Karim, F. D., Chang, H. C., Therrien, M., Wassarman, D. A., Laverty, T. and Rubin, G. M. (1996). A screen for genes that function downstream of Ras1 during Drosophila eye development. *Genetics* **143**, 315-329.

Kavaler, J., Duan, H., Aradhya, R., de Navas, L. F., Joseph, B., Shklyar, B. and Lai, E. C. (2018). miRNA suppression of a Notch repressor directs non-neuronal fate in Drosophila mechanosensory organs. *J. Cell Biol.* **217**, 571-583.

Kumar, J. P. (2012). Building an ommatidium one cell at a time. *Dev. Dyn.* **241**, 136-149.

Lai, E. C. (2002). microRNAs are complementary to 3′ UTR sequence motifs that mediate negative post-transcriptional regulation. *Nat. Genet.* **30**, 363-364.

Lai, E. C. (2015). Two decades of miRNA biology: lessons and challenges. *RNA* **21**, 675-677.

Lai, Z.-C. and Rubin, G. M. (1992). Negative control of photoreceptor development in *Drosophila* by the product of the *yan* gene, an ETS domain protein. *Cell* **70**, 609-620.

Lai, E. C. and Rubin, G. M. (2001). *neuralized* functions cell-autonomously to regulate a subset of Notch-dependent processes during adult *Drosophila* development. *Dev. Biol.* **231**, 217-233.

Lai, Z. C., Harrison, S. D., Karim, F., Li, Y. and Rubin, G. M. (1996). Loss of tramtrack gene activity results in ectopic R7 cell formation, even in a sina mutant background. *Proc. Natl. Acad. Sci. USA* **93**, 5025-5030.
Lai, E. C., Burks, C. and Posakony, J. W. (1998). The K box, a conserved 3′ UTR sequence motif, negatively regulates accumulation of *Enhancer of split* Complex transcripts. *Development* **125**, 4077-4088.
Lai, E. C., Tam, B. and Rubin, G. M. (2005). Pervasive regulation of Drosophila Notch target genes by GY-box-, Brd-box-, and K-box-class microRNAs. *Genes Dev.* **19**, 1067-1080.
Lee, Y. S., Nakahara, K., Pham, J. W., Kim, K., He, Z., Sontheimer, E. J. and Carthew, R. W. (2004). Distinct roles for drosophila dicer-1 and dicer-2 in the siRNA/miRNA silencing pathways. *Cell* **117**, 69-81.
Lewis, B. P., Burge, C. B. and Bartel, D. P. (2005). Conserved seed pairing, often flanked by adenosines, indicates that thousands of human genes are microRNA targets. *Cell* **120**, 15-20.
Li, X. and Carthew, R. W. (2005). A microRNA mediates EGF receptor signaling and promotes photoreceptor differentiation in the Drosophila eye. *Cell* **123**, 1267-1277.
Li, X., Cassidy, J. J., Reinke, C. A., Fischboeck, S. and Carthew, R. W. (2009). A microRNA imparts robustness against environmental fluctuation during development. *Cell* **137**, 273-282.
Luo, W. and Sehgal, A. (2012). Regulation of circadian behavioral output via a microRNA-JAK/STAT circuit. *Cell* **148**, 765-779.
Miska, E. A., Alvarez-Saavedra, E., Abbott, A. L., Lau, N. C., Hellman, A. B., McGonagle, S. M., Bartel, D. P., Ambros, V. R. and Horvitz, H. R. (2007). Most Caenorhabditis elegans microRNAs are individually not essential for development or viability. *PLoS Genet.* **3**, e215.
Mlodzik, M., Hiromi, Y., Goodman, C. S. and Rubin, G. M. (1992). The presumptive R7 cell of the developing Drosophila eye receives positional information independent of sevenless, boss and sina. *Mech. Dev.* **37**, 37-42.
Mohammed, J., Siepel, A. and Lai, E. C. (2014). Diverse modes of evolutionary emergence and flux of conserved microRNA clusters. *RNA* **20**, 1850-1863.
Monahan, A. J. and Starz-Gaiano, M. (2013). Socs36E attenuates STAT signaling to optimize motile cell specification in the Drosophila ovary. *Dev. Biol.* **379**, 152-166.
Schejter, E. D. and Shilo, B.-Z. (1989). The Drosophila EGF receptor homolog (DER) gene is allelic to faint little ball, a locus essential for embryonic development. *Cell* **56**, 1093-1104.
Schweitzer, R., Howes, R., Smith, R., Shilo, B.-Z. and Freeman, M. (1995). Inhibition of Drosophila EGF receptor activation by the secreted protein Argos. *Nature* **376**, 699-702.
Simon, M. A., Bowtell, D. D. L., Dodson, G. S., Laverty, T. R. and Rubin, G. M. (1991). Ras1 and a putative guanine nucleotide exchange factor perform crucial steps in signaling by the sevenless protein tyrosine kinase. *Cell* **67**, 701-716.
Smibert, P. and Lai, E. C. (2010). A view from Drosophila: multiple biological functions for individual microRNAs. *Semin. Cell Dev. Biol.* **21**, 745-753.
Smibert, P., Bejarano, F., Wang, D., Garaulet, D. L., Yang, J.-S., Martin, R., Bortolamiol-Becet, D., Robine, N., Hiesinger, P. R. and Lai, E. C. (2011). A Drosophila genetic screen yields allelic series of core microRNA biogenesis factors and reveals post-developmental roles for microRNAs. *RNA* **17**, 1997-2010.
Sun, K. and Lai, E. C. (2013). Adult-specific functions of animal microRNAs. *Nat. Rev. Genet.* **14**, 535-548.
Sun, K., Jee, D., de Navas, L. F., Duan, H. and Lai, E. C. (2015). Multiple in vivo biological processes are mediated by functionally redundant activities of *Drosophila mir-279* and *mir-996*. *PLoS Genet.* **11**, e1005245.
Tomlinson, A. and Ready, D. F. (1986). Sevenless: a cell-specific homeotic mutation of the Drosophila eye. *Science* **231**, 400-402.
Tomlinson, A. and Ready, D. F. (1987). Neuronal differentiation in Drosophila ommatidium. *Dev. Biol.* **120**, 366-376.
Tomlinson, A., Mavromatakis, Y. E. and Struhl, G. (2011). Three distinct roles for notch in Drosophila R7 photoreceptor specification. *PLoS Biol.* **9**, e1001132.
Truscott, M., Islam, A. B. M. M. K., Lopez-Bigas, N. and Frolov, M. V. (2011). mir-11 limits the proapoptotic function of its host gene, dE2f1. *Genes Dev.* **25**, 1820-1834.
Xiong, W. C. and Montell, C. (1993). tramtrack is a transcriptional repressor required for cell fate determination in the Drosophila eye. *Genes Dev.* **7**, 1085-1096.
Yoon, W. H., Meinhardt, H. and Montell, D. J. (2011). miRNA-mediated feedback inhibition of JAK/STAT morphogen signalling establishes a cell fate threshold. *Nat. Cell Biol.* **13**, 1062-1069.
Zelhof, A. C. and Hardy, R. W. (2004). WASp is required for the correct temporal morphogenesis of rhabdomere microvilli. *J. Cell Biol.* **164**, 417-426.